Seismic Performance of Light Wood Shear Wall Infilled Timber Frame Structures with Openings

Deshan Yang,[a,b,c,*] and Zhongfan Chen [a,b,c]

To study the seismic performance of wood frame structures filled with light wood shear walls, three full-size single-layer single span wooden frame structures with infill walls were designed and manufactured. The beams and columns were connected by mortise-tenon joints, and quasi-static tests were conducted on the specimens under reversed cyclic load. The failure modes and load-displacement hysteresis performance of structures with door opening infill wall, window opening infill wall, and solid infill wall were investigated. The seismic performance was analyzed using indicators such as strength, ductility, and equivalent viscous damping ratio. The failure modes of light wood frame filling walls were the tearing of sheathing panel and the failure of nail connections. The filled wall with the opening initially exhibited inclined cracks at the corner of the opening, and then they extended to the periphery. Compared with the solid filled wall, the positive and negative bearing capacity of the structure with door opening decreased, and that of the structure with window opening decreased also. Because the specimens with opening in the filled wall were more conducive to the deformation of the structure when the bearing capacity was not significantly reduced, the ductility of the specimen with door opening was the highest.

DOI: 10.15376/biores.19.2.2916-2934

Keywords: Light wood infill wall with opening; Timber frame; Full-scale quasi-static experiment; Hysteretic behavior; Ductility

Contact information: a: Key Laboratory of Concrete and Pre-stressed Concrete Structures of the Ministry of Education, Southeast University, 02, Southeast University Road, Nanjing 211189 P.R. China; b: School of Civil Engineering, Southeast University, 02, Southeast University Road, Nanjing 211189 P.R. China; c: China-Pakist Belt and Road Joint Laboratory on Smart Disaster Prevention of Major Infrastructures, Southeast University, 02, Sipailou, Nanjing 210096 P.R. China;
** Corresponding author: 15251836139@163.com*

INTRODUCTION

After thousands of years of development, Chinese traditional wood architecture has achieved brilliant achievements, such as Yingxian Wood Pagoda, which still stands today. These excellent wooden structures are important symbols of Chinese civilization and have profoundly influenced the architectural styles of East and South Asia. The beams and columns of the traditional Chinese wooden structure are connected to each other through mortise-tenon joints and are filled with masonry, leaving a gap between the filling wall and the wooden column to reduce the earthquake effect. Due to the serious deformation and deterioration of energy dissipation capacity of masonry filling walls, brittle failure occurs in earthquakes and leads to structural collapse. Therefore, a light wood shear wall is used as a filling wall in this study to make up for the shortage of traditional filling wall materials. The presence of an opening can significantly change the force transmission path of a

structure, so the effects of window openings and door openings on the seismic performance of a structure were investigated in this paper.

Pan *et al*. (2020) analyzed the force mechanism of the through-tenon joint. They used the numerical analysis software ABAQUS to establish a three-dimensional solid model of the through-tenon joint. The correctness of the numerical model was verified by pseudo-static test results, and then the effects of joint gap, transverse elastic modulus, and tenon length on the mechanical properties of joints were analyzed (Pan *et al*. 2020). The mechanical model of through-tenon joint was divided into slip section, elastic section, and yield section, and the test results of the through-tenon joint were compared with the moment-angle mechanical model of the through-tenon joint to verify the correctness of the mechanical model (Pan *et al*. 2020, 2023).

The columns of traditional wooden structures are often placed on the foundation by means of flat swing floating shelves. Because there is no fixed constraint, under the action of earthquakes they can only withstand pressure but not tension, and the column feet are repeatedly lifted, which is similar to the motion form of swaying columns. According to the compression state when the column foot has entered the plastic state, the swaying process of the wooden column could be divided into full section elastic swaying, small section elastic-plastic swaying, large section elastic-plastic swaying, and full section elastic-plastic swaying. The moment-rotation relationship of the column foot during the swaying process could be obtained through the geometric conditions and force balance conditions (Pan *et al*. 2022; An *et al*. 2023).

Based on the transverse compression deformation characteristics of wood and the assumption of orthotropic anisotropic properties of materials, Yu (2022) derived the mechanical models of half-tenon, through-tenon, and joint dowel joints. Then the stiffness matrix of mixed elements was prepared, including mortise and tenon joints and column feet. Considering the friction-slip-contact behavior of mortise and tenon joints and the rotation behavior of column feet, Yu *et al*. (2021, 2022a) established the beam element model of a single span wooden frame. The anti-lateral movement principle of the wooden frame was analyzed, and the dynamic analysis of the wooden frame was carried out (Yang *et al*. 2020). The research showed that the mechanical properties of the frame were closely related to the contact state of the half-tenon joint and the column foot joint (Yu *et al*. 2021; Yu 2022). The joint gap in the half-tenon wood frame weakens the anti-lateral displacement ability of the frame obviously, and the anti-lateral displacement stiffness of the half-tenon wood frame increases with the length of the tenon (Yu *et al*. 2021; Yu 2022). During the oscillating process of the wooden frame, the kinetic energy and gravitational potential energy are exchanged back and forth, and the input energy is finally transformed into unrecoverable damping and friction energy consumption (Yu *et al*. 2022b).

Some scholars have improved the seismic performance of traditional wooden structures by strengthening mortise and tenon joints. Li (2018) used detachable non-destructive flat steel and FRP to strengthen mortise and tenon joints, and the research results showed that the flat steel reinforced joints still showed semi-rigid characteristics. In the initial stage of loading, the FRP-reinforced nodes were tightly wrapped, so that the rotation of the nodes was completely limited, and the rotational stiffness of the nodes was very large, which basically showed the mechanical performance of the rigid nodes. Due to the relative sliding between flat steel and joint and the yield of flat steel, the flat section of the moment-rotation angle curves of flat steel reinforced joints was longer than that of unreinforced joints, and the secant stiffness of joints after steel hoop reinforcement was much larger than that of unreinforced joints. The non-destructive reinforcement of flat steel

had a significant effect on controlling the amount of tenon pulled out (Li *et al*. 2021).

Guo (2022) actively explored the mechanical properties improvement technology of the Chuan-Dou style wooden structure. A reinforcement scheme with self-tapping screws for the exterior straight mortise-tenon joint was proposed. The influence of the yield strength and diameter of self-tapping nails on the flexural performance of reinforced joints was studied by numerical simulation. The numerical simulation results showed that the yield strength of the self-tapping nails had little effect on the flexural performance of the reinforced joints. With the increase of the diameter of the self-tapping screws, the flexural stiffness and flexural capacity of the joints increased. It was recommended that self-tapping screws with a diameter of 8 mm be used as pin reinforcing parts for the exterior straight mortise-tenon joints (Guo *et al*. 2022).

Xu *et al*. (2015) conducted a low-cycle repeated load test on the wooden frame with brick filling walls. After adding brick filling walls, the lateral bearing capacity and stiffness during forward pushing were significantly improved, and the stage energy consumption during forward pushing was also significantly higher than that of the empty frame.

The sheathing panel materials of light wood structure wall are generally wood plywood, OSB board, *etc*. With the continuous improvement of bamboo board processing industry, the application of bamboo plywood to wood shear wall has broad development prospects. Light wood construction requires extensive use of metal connectors to form a continuous force transmission path. Wang (2019) conducted the corresponding experimental research on the metal connector system. The bending yield strength was obtained for the three types of nails commonly used in glubam structure through the bending resistance test. The load-carrying capacity of the frame-frame connection with high strength nails is higher than that of the ordinary nail connection. The hold-down anchorage connection suitable for glued bamboo light frame shear wall was designed, and the hold-down connection with two kinds of bearing capacity was experimentally studied (Wang *et al*. 2019).

As an important lateral force resisting component in earthquake, the mechanical properties of bamboo plywood panel light wood shear wall are very important. Through the monotonic and hysteretic tests, the unit length bearing capacity, secant modulus, and ductility coefficient of the wall were obtained, and the seismic performance of the wall was determined to be good (Wang *et al*. 2017). The use of round jet nails and steel row nails can meet the requirements of industrial processing at present, such that the structure can meet the requirements of the design value of bearing capacity of ordinary wood-based structural plate shear wall with the same thickness (Li *et al*. 2013).

The deformation of the floor is relatively small in the plane of the actual light wood structure house under eccentric load, which is close to the rigid diaphragm. The wall perpendicular to the direction of load has an obvious effect on limiting the rotation and deformation of the floor. The rotating deformation components of the floor were very small, and the floor was approximately rigid translation in the process of load distribution and transfer (Chen 2009; Chen *et al*. 2010).

The lateral shear load in the plane of the light wood frame shear wall is transferred to the sheathing panel through the upper and lower borders of the shear wall, and the shear load is mainly borne through the sheathing panel. The nail joints connecting with the wall frame along the periphery of the sheathing panel play an important role in bearing the lateral shear load. Chen *et al.* (2008) conducted lateral shear tests of ordinary round nail joints, and the research showed that the joint strength of nails was greatly affected by the edge distance. When the nail was pulled out, the bearing capacity of the specimen was the

highest and the ductility was the best. By contrast, when the standard wood was subjected to compressive failure, the bearing capacity of the specimen was the lowest. The bearing capacity of the specimens torn at the edge of plate and the specimens torn at the edge of specification wood was poor, which was due to brittle failure. Through the monotone loading test of light wood structure shear wall and the finite element analysis software ABAQUS to simulate the mechanical performance of the shear wall, it was confirmed that the bearing capacity and stiffness of the shear wall were approximately linear with the wall length, and the rotation deformation of the narrow plate was large and easy to be destroyed (Chen *et al*. 2011).

Under the action of horizontal load, the nails of ordinary light wood shear walls are prone to penetration, shearing, and pulling out damage, resulting in reduced bearing capacity. Zheng *et al*. (2016a) conducted a horizontal lateral force resistance test of sheathing sandwiched wood shear walls, and studied the effects of the wall length, stud spacing, the thickness of sheathing panels and the spacing of nails on the lateral resistant performance.

In the sheathing sandwiched wood shear wall, the influence of double shear nailing joints on edge wall bones such as top beam plate, bottom beam plate, end wall bone column and common wall bone column was the most critical, and the anti-shear properties of double shear nailing joints were also affected by plate end distance, plate thickness and loading direction (Zheng *et al*. 2016b).

In order to avoid the damage of conventional sheathing sandwiched wood shear wall edge tearing and nail pulling out, the wood-based structural plate was replaced by a plybamboo panel with higher strength. Under the action of low cyclic load, fatigue shear failure of self-tapping screws occurred in midply of the bamboo shear wall (Zheng *et al*. 2023).

Xia *et al*. (2022) calculated the damage index based on the damage model of the component hysteretic energy consumption to evaluate the damage of the bamboo plywood shear wall. Zheng *et al*. (2021) used self-tapping screws in the bamboo plywood shear wall. They explored the accumulation law of damage through the experimental study of this kind of double-shear screw connection

The ultimate bearing capacity of double-shear screw connection of plybamboo panel is higher than that of conventional double-shear screw connection with wood-based structural plate and bamboo as the center. Therefore, replacing wood-based structural plate and conventional nail connection with plybamboo panel and self-tapping screws is helpful to improve the lateral force resistance of midply shear wall (Zheng *et al*. 2020; Dong *et al*. 2023).

As the failure of the sheathing panels of light wood shear walls was concentrated at the bottom and top, Di (2019) used SPF timber plates and bamboo scrimber panels with good performance at the top and bottom of the shear walls, and OSB boards were still used in the middle of the sheathing panels. The sheathing-to-framing joints test and reliability analysis were carried out, and the monotonic loading test was carried out on the reinforced light wood shear walls with narrow panels at the end (Di and Zuo 2021a,b,c; Zuo and Di 2021; Di 2023). It was observed that the use of bamboo scrimber panels can improve the ultimate bearing capacity of traditional light wood frame shear walls, and the specimens with self-tapping nails have the greatest reinforcement effect (Di 2019).

In this work, the light wood shear wall was filled in the wood frame with mortise and tenon joints. The frame and light wood shear wall jointly bear the lateral shear force, improving the overall lateral performance of the structure. The timber frame-light-wood

shear wall structure solves the problem of low lateral stiffness in traditional wood frame structures, enhances the overall strength and stiffness of the structure, and can also play a role in enclosure and separation. It is an economical, practical, and high-strength structural system. This structure can effectively combine the advantages of wood frames and light wood shear walls, achieving green environmental protection, economic efficiency, and has broad application prospects in future wooden structure buildings. As for the current situation, the research on timber frame-light-wood shear wall structural system is still in the preliminary stage, and the cooperative working mechanism and failure characteristics of wood frame-light-wood shear wall structure are not clear, so it is necessary to carry out further analysis and research on the lateral resistance performance of wood frame-light-wood shear wall structure. The failure mode, hysteretic curve, skeleton curve, and energy dissipation capacity of the three specimens were compared and analyzed by full scale low cycle reciprocating seismic performance test, which had important theoretical significance and application value for improving the lateral resistance performance of traditional wood structures.

EXPERIMENTAL

Design and Fabrication of Specimens

The diameter of the wood frame column was 200 mm, and the height was 3200 mm. The cross-section size of the beam was 200 × 120 mm and the beam length was 3000 mm. The light wood shear wall stud was composed of 38 mm × 89 mm specification materials. The top beam plate and the bottom beam plate were made of structural lumber, and the cross-section size was 38 mm × 89 mm. Each end of the wall stud was connected with the bottom beam plate and the top beam plate with 3.8 mm × 80 mm nails. The stud spacing of solid shear wall was 400 mm, and the stud spacing of shear wall with opening was 350 mm. The 9 mm thick oriented strand board (OSB) sheathing was fastened to the stud by 2.8 mm × 50 mm nails. The 12 mm thick gypsum wallboards (GWB) was fastened to the wall stud by wood screws with a diameter of 3.5 mm and a length of 38 mm. The nail connection between the sheathing panel and the wall stud was arranged along the center line of the wall stud. When the adjacent sheathing panels were connected to the same wall stud, the nail distance from the sheathing panel edge was 10 mm. The nail spacing on the edge of sheathing panel was 150 mm and the nail spacing in the field was 300 mm. The end face of the nail head was flush with the sheathing panel. The size of the sheathing panel was 1.2 m×2.4 m. In actual building structures, infill walls often have door and window openings, and the presence of these openings changes the force transmission path of the infill wall, affecting its mechanical behavior and significantly affecting the seismic performance of the structure. Considering the influence of openings, three full-scale specimens were designed, with specific structural characteristics shown in Table 1 and schematic diagrams shown in Fig. 1.

Table 1. Specimen Number and Structural Characteristics

Specimen Number	Size of Infill Wall (m x m)	Sheathing Thickness (mm)	Sheathing Material
FLiO-1	2.4 x 2.4 with 1.0 x 2.0 door opening	9	OSB
FLiO-2	2.4 x 2.4 with 1.0 x 1.0 window opening	9	OSB
FLiG	2.4 x 2.4	9/12	OSB/GWB

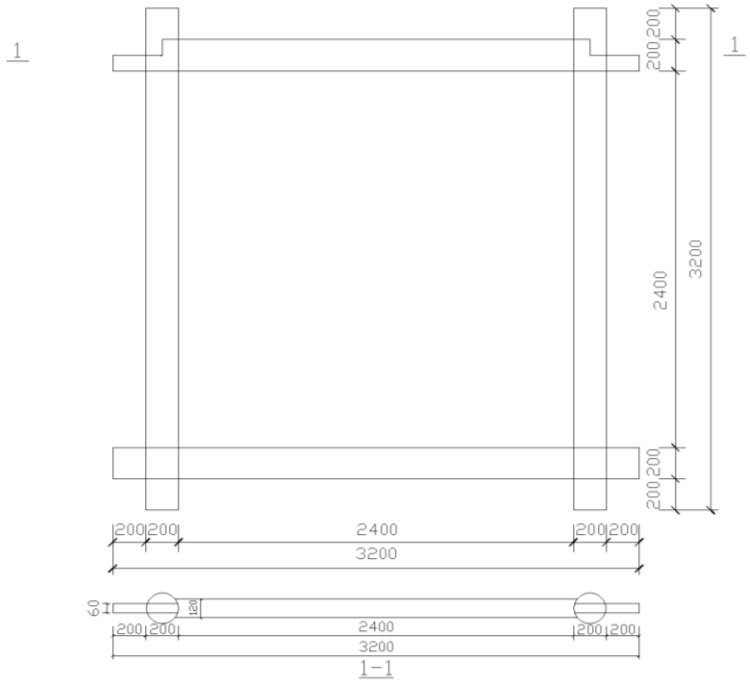

(a)

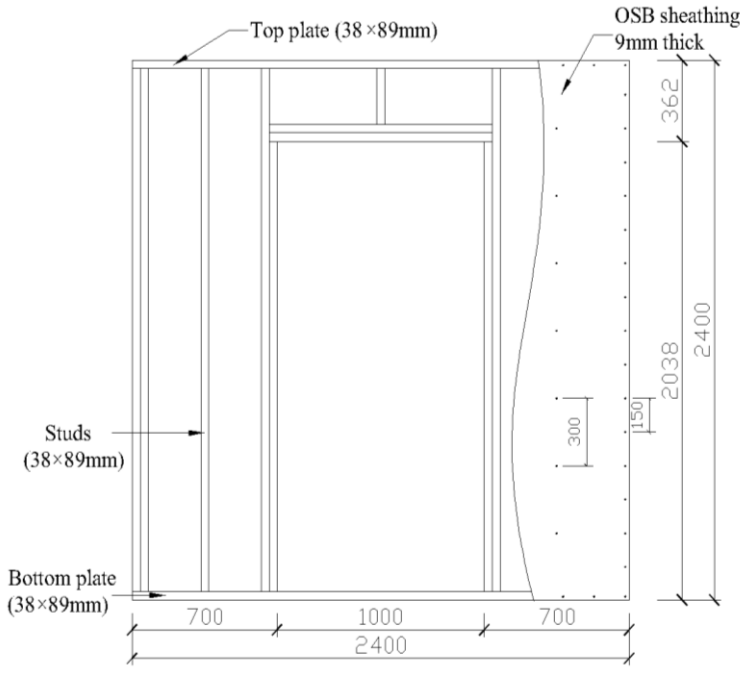

(b)

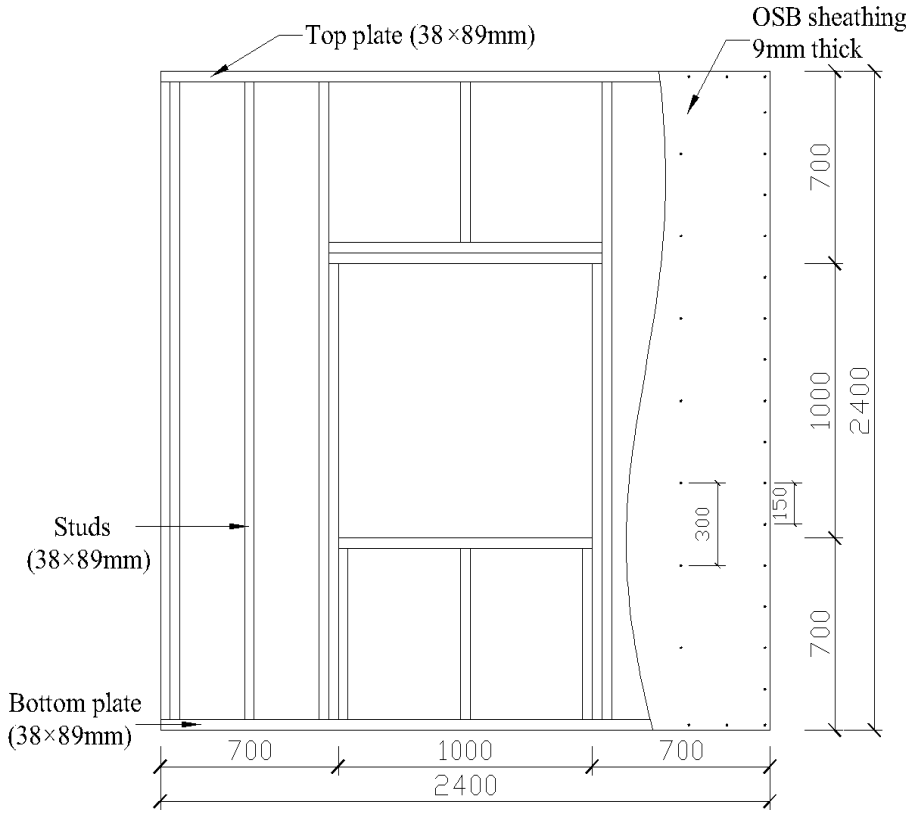
Top plate (38×89mm)
OSB sheathing
9mm thick
Studs
(38×89mm)
Bottom plate
(38×89mm)
700
1000
700
2400
300
150
700
1000
2400

(c)

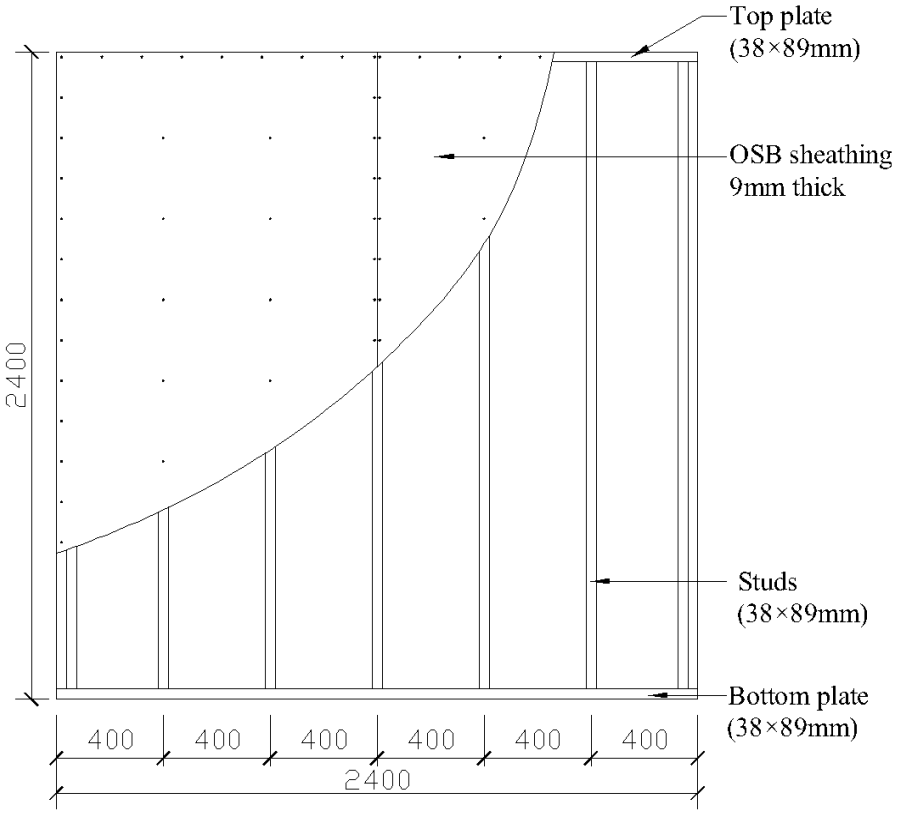
Top plate
(38×89mm)
OSB sheathing
9mm thick
Studs
(38×89mm)
Bottom plate
(38×89mm)
2400
400
400
400
400
400
400
2400

(d)

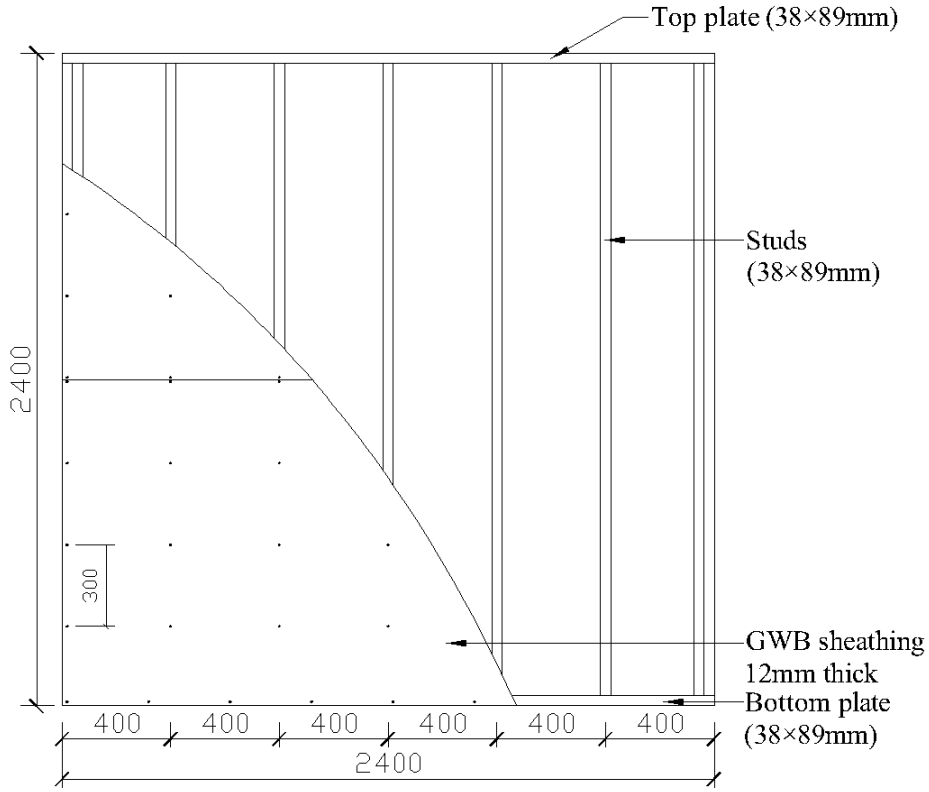

Fig. 1. Structure diagram of the specimen: (a) Exterior wood frame; (b) FLiO-1: Infill wall with door opening; (c) FLiO-2: Infill wall with window opening; (d) FLiG: Solid fill wall on OSB panel side; (e) FLiG: Solid fill wall on GWB panel side (all dimensions are in mm)

Test Setup and Loading Regime

In the experiment, hinge supports were manufactured and placed at the bottom of the column. The hinge supports were fixed in the laboratory trench by anchor bolts. The vertical load was applied to the top of the column by manual hydraulic jacks, and the vertical jacks were connected to the beam of the reaction frame by sliding trolley, which could ensure that the acting position of the axial force on the specimen was unchanged. The applied axial force was 10 kN. The horizontal load was applied by a hydraulic actuator fixed to the reaction wall, and the specimen was connected to the horizontal actuator by a steel tie rod. In order to prevent out-of-plane instability during loading, steel lateral supports were applied on the outside of the frame plane. The test setup and the overview of the specimen are shown in Figs. 2 and 3.

The method of low-cycle repeated loading was adopted, and the loading was controlled by displacement. The initial value of loading was 10 mm, and the displacement increase of each stage was 10 mm. Each stage of displacement was cyclic loaded 3 times, and the displacement was increased step by step until the specimen was damaged or not suitable for loading.

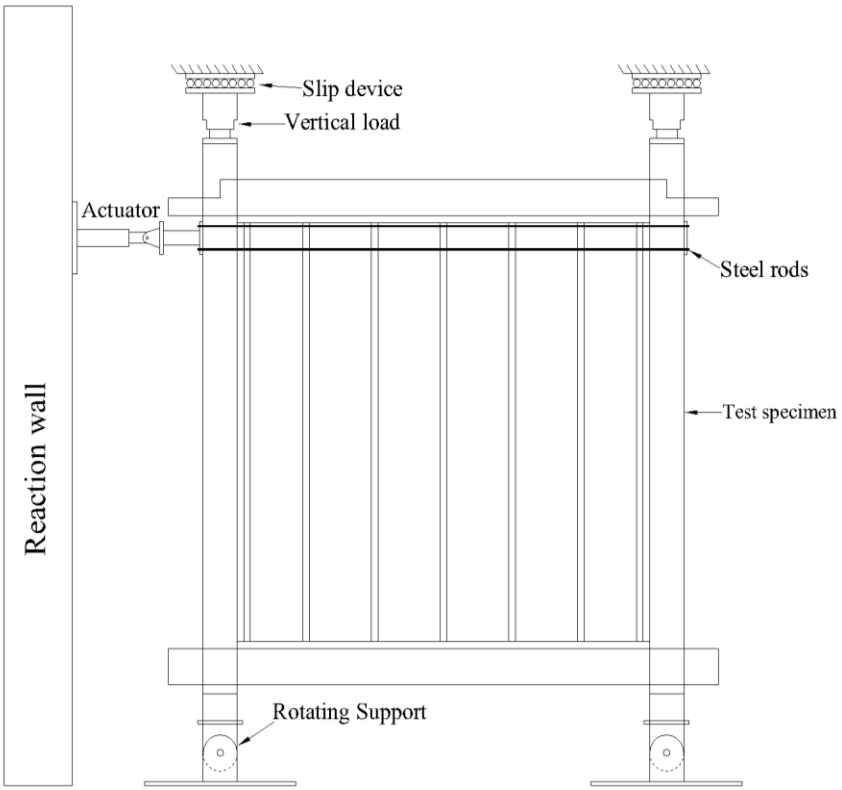

Fig. 2. Quasi-static test setup

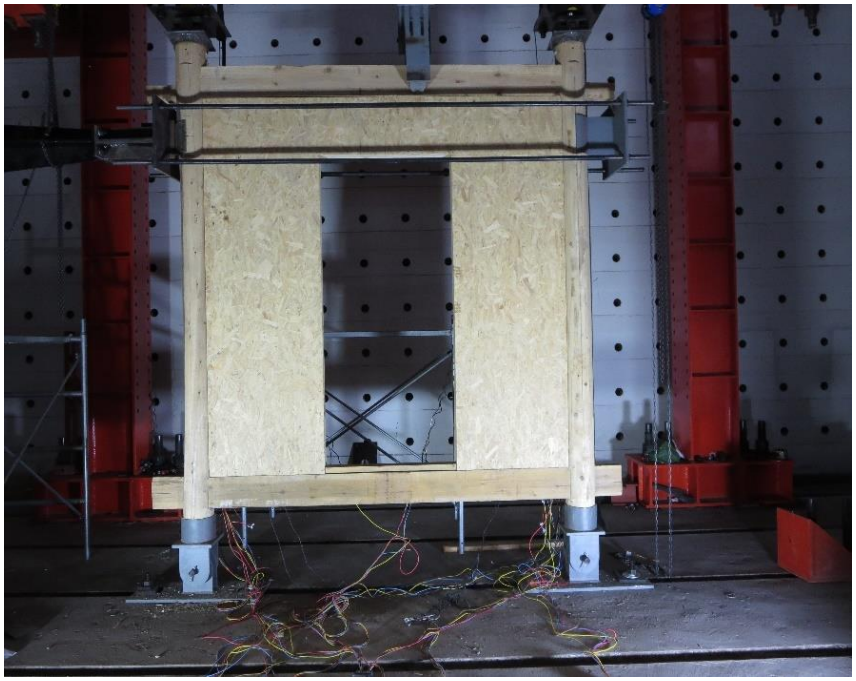

Fig. 3. Overview of the specimen

RESULTS AND DISCUSSION

Failure Modes

The failure phenomena of the specimens are shown in Fig. 4. For specimen FLiO-1, with the increase of load, the OSB plate rotated relatively greatly. Individual nail connections were concave into the OSB plate. The two upper corner points of the door opening were subjected to tensile stress and compressive stress respectively, resulting in two types of damage: tearing and buckling of the sheathing panel. Due to the large opening area, the average stress borne by the sheathing panel was large. In the process of low-cycle repeated load, some nails at the edge of the sheathing panel were destroyed, and more nails in the central part of the panel were also damaged. The whole panel had obvious in-plane rotation. Cracks appeared at the two upper corners of the opening, slanting upwards to the left and upwards to the right, and gradually extended to the top of the wall.

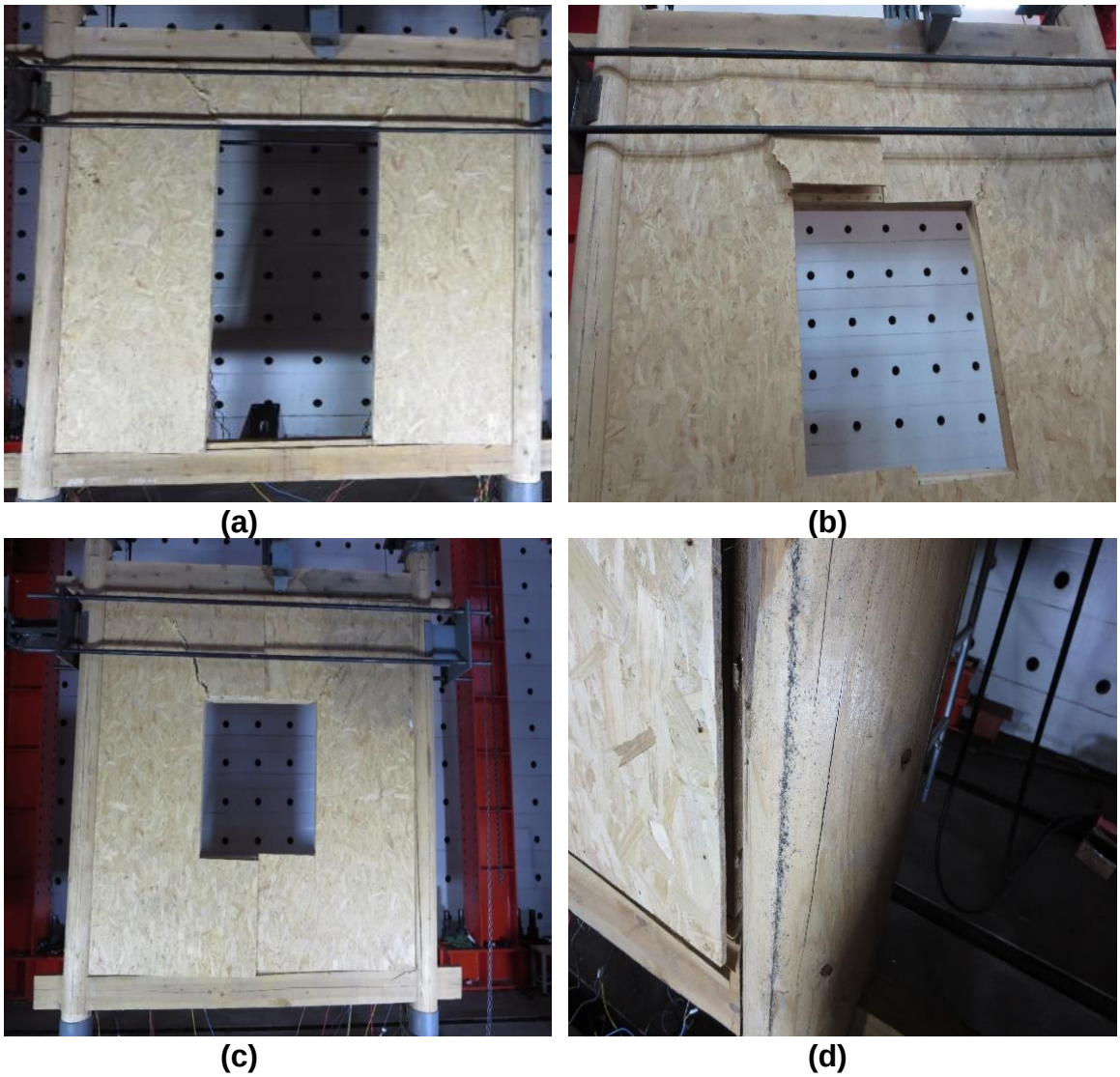

Fig. 4. Typical failure modes of specimen: (a) Diagonal cracks at the top of the door opening; (b) Diagonal cracks on the upper part of the window opening; (c) OSB board misalignment**;** (d) The nails penetrated through the sheathing panel

For specimen FLiO-2, during the loading process, the cracks at the two upper corners of the opening slanted upward to the left and upward to the right through to the top. The splice of the sheathing panel had a large lifting, the OSB board near the window opening was penetrated by nail caps, and the nails were slightly pulled out. The sheathing panel exhibited damage phenomena such as tensile tearing and bulging under compression.

For the specimen FLiG, the gypsum board was damaged before the OSB board, and the damage of the gypsum board first occurred at the intersection of two gypsum boards. Due to the softness and brittleness of the gypsum board, some parts were penetrated by screws. As the loading displacement increased, the nails at the edge of the OSB board penetrated the wall board, and some nails were slightly pulled out. In the late loading period, the OSB board exhibited a greater degree of mutual dislocation, and a portion of the nail connections in the middle of the board became embedded in the panel. The failure of shear wall was mainly due to the failure of nail connections.

Hysteretic Characteristics

The hysteresis curves of the specimens are shown in Fig. 5. With the increase of loading displacement, the nail connections in shear wall were degraded and destroyed gradually, and the pinching effect of the hysteresis loops became more apparent. The hysteresis loops showed clear Z-shape.

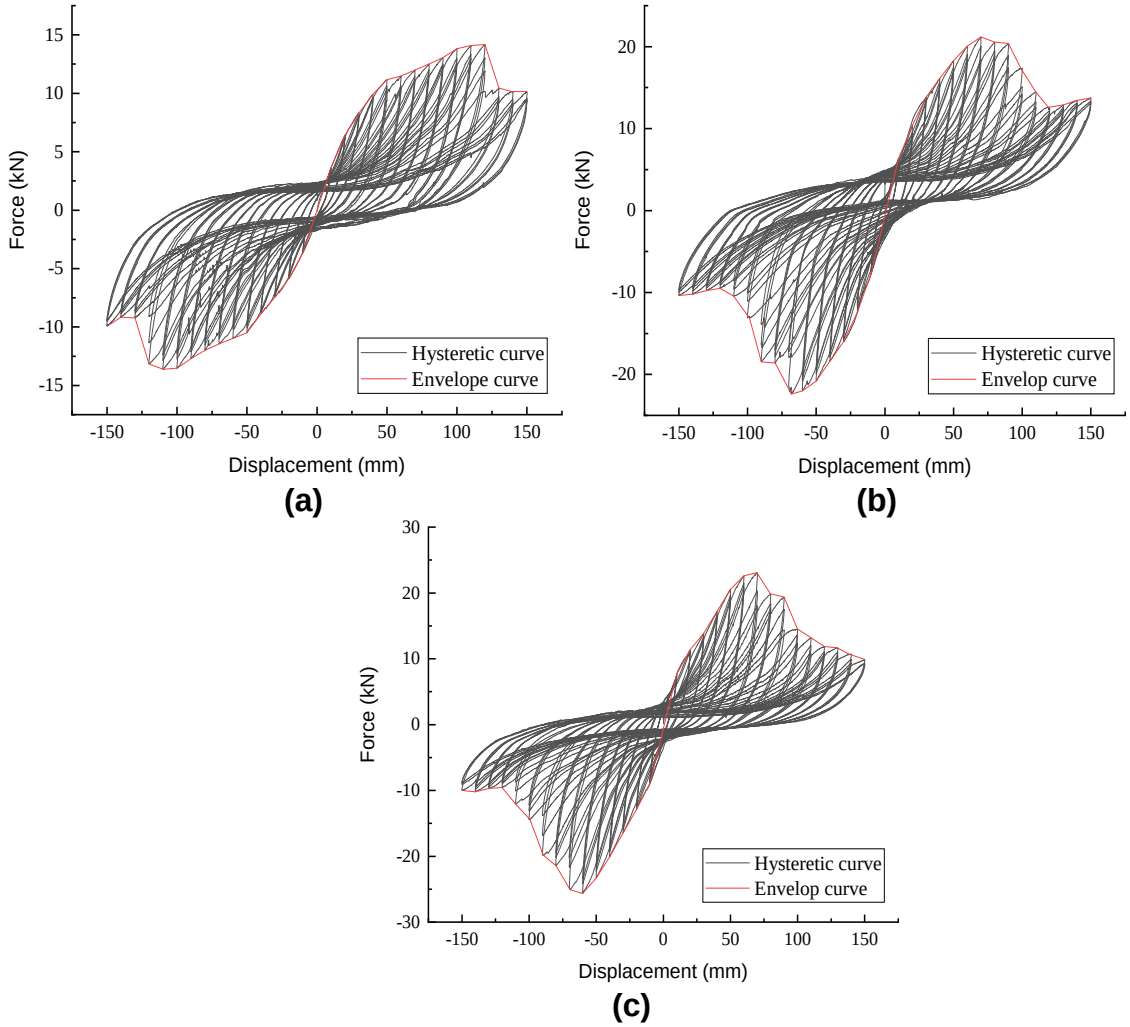

Fig. 5. Hysteretic and envelope curves: (a) FLiO-1; (b) FLiO-2; and (c) FLiG

When the horizontal displacement was very small, the specimens were in the elastic stage, and the load increased linearly with the displacement. After unloading, within this stage, the deformation could basically be completely restored. When the displacement increased, the load-displacement curve gradually deviated from the straight line, and the deformation accelerates. After unloading, the displacement couldn't be completely restored, exhibiting a certain degree of plasticity. After multiple repeated loading, the nail connection between the wall stud and the sheathing panel would slip and gradually entered the elastoplastic state. Under the same level of control displacement, the strength damage of the component caused by cyclic loading resulted in an overall decrease in the hysteresis loop for each additional cycle.

The peak bearing capacity of the filled wall specimen with openings had decreased to different degrees compared to the specimen with solid filling. The presence of the door opening reduced the bearing capacity of specimen FLiO-1 by 38.6% and 46.9% in both positive and negative directions compared to the solid filled wall FLiG, respectively. The presence of window opening reduced the bearing capacity of specimen FLiO-2 by 8.2% and 12.7% in both positive and negative directions compared to the solid filled wall FLiG, respectively.

Stiffness Degradation

The variation law of lateral stiffness of a structure under reciprocating cyclic loading is an important basis for studying its seismic performance, the stiffness variation can be described by the secant stiffness K_i, as shown in equation (1):

$$K_i = \frac{|+F_i|+|-F_i|}{|+\Delta_i|+|-\Delta_i|} \quad (1)$$

where F_i represents the peak load of the i-th cycle, and Δ_i represents the target displacement of the i-th cycle. The stiffness degradation of the specimen is shown in Fig. 6.

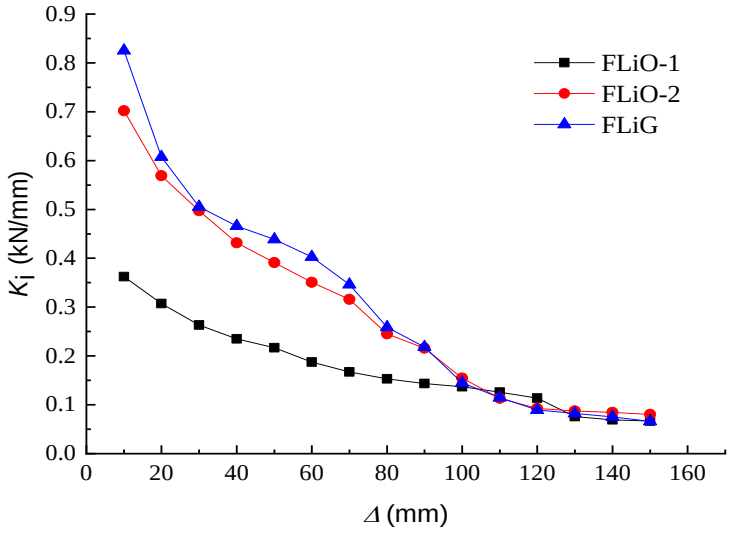

Fig. 6. Stiffness degradation curves

Figure 6 shows the comparison of secant stiffness degradation of each specimen. The relationship curve between secant stiffness and lateral displacement at each loading grade can reflect the speed of stiffness degradation of each specimen. It can be clearly seen that compared with the other two specimens, the secant stiffness degradation of specimen

FLiG was the fastest, because the solid filling wall experienced sharp damage in a short time. The larger the opening size, the greater the deformation capacity of the wall limb, and the lower the lateral stiffness of the specimen. The presence of a door opening in specimen FLiO-1 reduced the initial stiffness of the structure by 56.1% compared to the solid filled wall specimen FLiG. Compared with specimen FLiG, the initial stiffness of specimen FLiO-2 decreased by 15.0%, indicating that the presence of the opening had a significant impact on the structural stiffness.

When the lateral displacement was greater than 100 mm, the slopes of the three curves tended to be parallel, indicating that the stiffness degradation rate was basically consistent. This is because at this time, the damage of the filled wall has been so serious that it can hardly provide any lateral stiffness, and the stiffness degradation was mainly caused by the stiffness damage of the timber frame.

Strength Degradation Law

During the same level loading process, the structural bearing capacity decreases with the increase of cycle number, and the strength degradation is expressed by the ratio of peak bearing capacity η_i. The strength degradation curve under each displacement amplitude is shown in Fig. 7. As shown in Fig. 7, all specimens exhibited the phenomenon of strength degradation, and the strength degradation coefficient was above 0.8. The reason for this is that under the same level of controlled displacement, the plastic deformation of the nails in the specimen mainly occurred in the first loading process, and only when the specimen experienced a larger displacement, new plastic deformation occurred. Therefore, during the second cycle of loading, there was a certain degree of decrease in horizontal load. Overall, the strength degradation of wood frames with infill walls was less than 20%, which showed good seismic performance in terms of strength degradation.

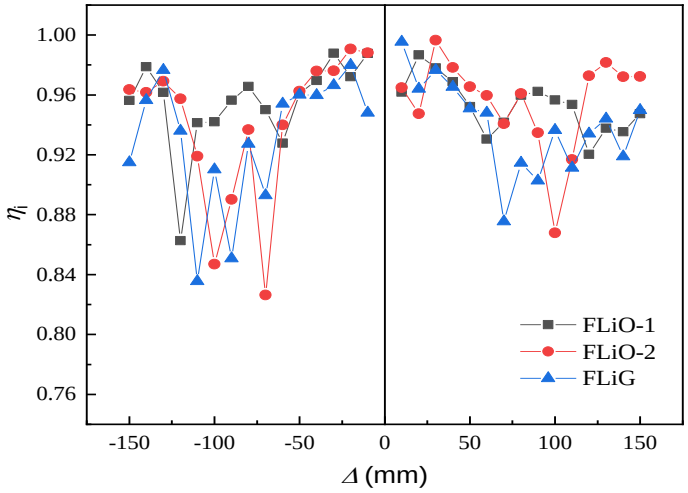

Fig. 7. Strength degradation curves of specimens

Equivalent Viscous Damping Coefficient

During the loading process, the area surrounded by the *P-Δ* hysteresis curve reflects the magnitude of the energy absorbed by the structure. During the unloading process, the total area surrounded by the unloading curve and the loading curve reflects the magnitude of the dissipated energy of the structure. The equivalent viscous damping coefficient ζ_{eq} is

used to quantitatively evaluate the energy dissipation capacity of the structure. The equivalent viscous damping coefficient ζ_{eq} can be calculated as follows,

$$\zeta_{eq} = \frac{1}{2\pi}\frac{S_{ABC}+S_{CDA}}{S_{OBE}+S_{ODF}} \quad (2)$$

where $S_{(ABC+CDA)}$ is the rea surrounded by the hysteresis curve in Fig. 8 and $S_{(OBE+ODF)}$ is the sum of areas of the triangle OBE and ODF in Fig. 8.

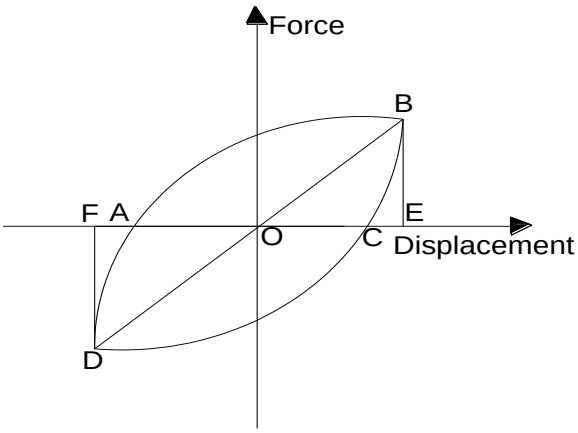

Fig. 8. Calculation method of equivalent viscous damping coefficient

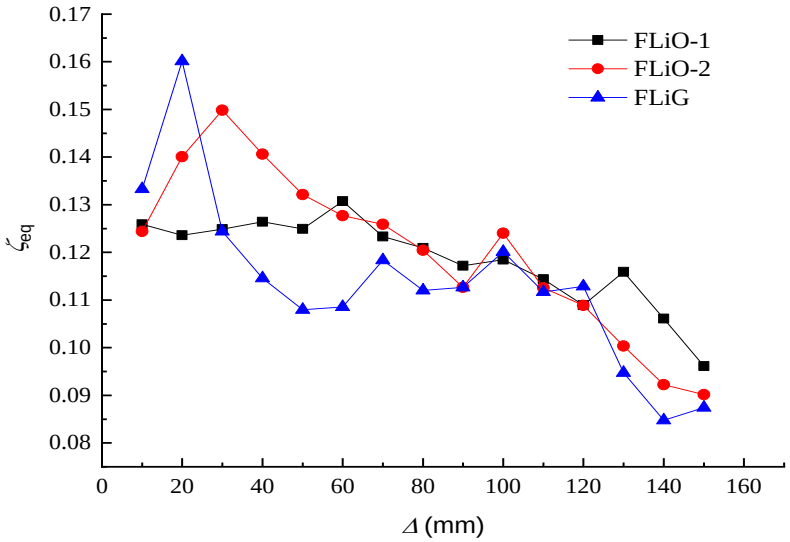

Fig. 9. Equivalent viscous damping coefficient

As shown in Fig. 9, with the increase of loading displacement, the equivalent viscous damping coefficient of wood frames with filled walls decreased significantly on the whole, which was reflected in the evolution process of hysteresis loops of each specimen under different loading displacements. When the displacement was small, the hysteresis loops were spindle-like and exhibited high energy dissipation efficiency. With the increased of the loading displacement, the hysteresis loop gradually evolved into the inverse S-shaped form and eventually becoming Z-shaped. The pinching effect of hysteresis loops became more and more obvious, and the energy dissipation efficiency decreased gradually. The filling of the light wood shear wall hindered the deformation of

the wood frame. In the early stage when the loading displacement was small, it was affected by the filling wall with relatively high stiffness. In this case, the deformation of the nail connections in the light wood shear wall was the main mechanism for energy consumption of the specimen.

Ductility

The displacement ductility coefficient of a structure refers to the ratio of ultimate displacement Δ_u to yield displacement Δ_y, which can be used to evaluate the deformation capacity of the structure. The yield point can be calculated by using the EEEP (Equivalent Energy Elastic Plastic) curve, where the area A_1 is equal to the area A_2, as shown in Fig. 10.

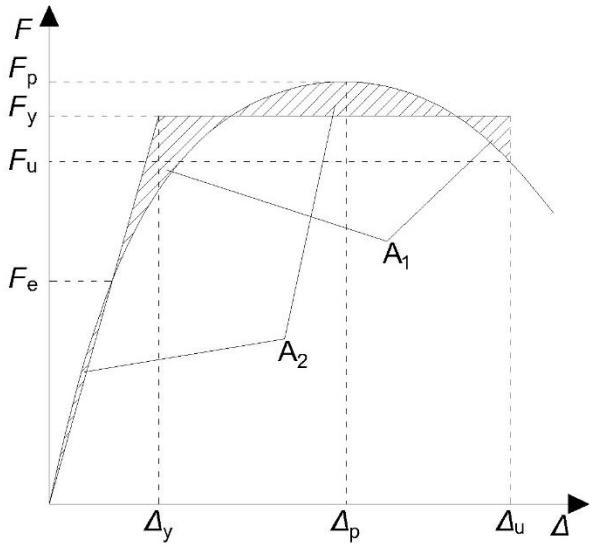

Fig. 10. EEEP curve

Table 2. Ductility Value of Each Specimen

Specimen	Δ_y(mm)	Δ_u(mm)	μ	$\mu_{Average}$
FLiO-1	37.3	127.54	3.42	3.33
	-38.92	-125.72	3.23	
FLiO-2	33.69	100.59	2.99	3.16
	-27.33	-90.86	3.32	
FLiG	29.99	91.86	3.06	3.03
	-28.41	-85.28	3	

The calculation results of the ductility coefficients of each specimen are shown in Table 2. According to the data in the table, the FLiG specimen with solid infill wall had the worst ductility and lower ultimate displacement. The FLiO-2 specimen with a door opening filled wall had the highest ductility coefficient, which was because the specimen with an opening in the filled wall was more conducive to structural deformation when the bearing capacity was not significantly reduced. The ductility coefficient of the specimen was between 3.03 and 3.33, indicating good ductility. Under earthquake action, the structure can generate certain plastic deformation to consume seismic energy.

CONCLUSIONS

1. Due to the stress concentration in the corner of the opening, the sheathing panel of the light wood shear wall specimen with opening would be torn or crushed. At the two upper corner points of the opening, large cracks occurred along the slope to the upper left and the slope to the upper right, and they gradually extended to the top of the wood shear wall.
2. The opening of the wall significantly weakened the bearing capacity, and the bearing capacity of specimen FLiO-1 was 38.6% and 46.9% lower than that of solid filled wall specimen FLiG in both positive and negative directions, respectively. The presence of window opening made the bearing capacity of specimen FLiO-2 lower by 8.24% and 12.7% than that of solid filled wall specimen FLiG in both positive and negative directions, respectively. For positions where openings are not necessary, it is best not to make openings in the wall, especially for large-sized openings, to avoid excessive weakening of bearing capacity.
3. The stiffness variation trend of all specimens was roughly the same, and the stiffness degradation was faster in the early stage of loading. The opening of the infill wall significantly weakened the stiffness, and the initial stiffness of specimen FLiO-1 was 56.1% lower than that of the solid infill wall specimen FLiG. Compared with specimen FLiG, the initial stiffness of specimen FLiO-2 decreased by 15.0%.
4. All specimens showed a phenomenon of strength degradation, with strength degradation less than 20%, and the overall degradation amplitude was relatively small. Changes in the size of openings could alter the ultimate displacement and energy dissipation of the structure. As the loading displacement increased, the equivalent viscous damping coefficient of wood frame structure with infill walls decreased significantly overall.
5. The ductility coefficient of the specimen was between 3.03 and 3.33, indicating good ductility. Because the presence of openings in the infill wall was more conducive to structural deformation when the bearing capacity didn't significantly decrease, the ductility coefficient of specimen FLiO-2 was higher than that of specimen FLiG with solid infill wall.
6. When timber frame-light-wood shear wall structural system is subjected to horizontal force, the main failure occurs at the nail joint of the wood shear wall. Because the lateral stiffness of the wood shear wall is much higher than that of the wood frame, the wood shear wall bears the main horizontal force. In the case of large deformation, the external frame can effectively inhibit the lifting of the wall stud at the end of the shear wall, so it is not necessary to install hold-down connectors in the shear wall. This study provides a theoretical reference for guiding the design and application of such structures and promotes the development and application of this structural system.

ACKNOWLEDGMENTS

This research was supported by the National Key R&D Program of China (No. 2018YFD1100402).

REFERENCES CITED

An, R., You, W., Pan, Y., and Fan, Y. (2023). "Static and dynamic analyses of traditional Chinese timber columns under horizontal accelerations," *Structures* 47, 37-51. DOI: 10.1016/j.istruc.2022.11.043

Chen, S., Chen, Z., Fan, C., Pan, J., and Wang, H. (2008). "Experimental study on nail fasteners in wood shear walls," *Acta Scientiarum Naturalium Universitatis Sunyatseni* 47(4), 133-138. (in Chinese)

Chen, S. (2009). *Behavior of Light Wood Frame Construction under Wind Load*, Ph.D. Dissertation, Harbin Institute of Technology, Harbin, China. (in Chinese)

Chen, S., Fan, C., and Pan, J. (2010). "Experimental study on full-scale light frame wood house under lateral load," *Journal of Structural Engineering* 136(7), 805-812. DOI: 10.1061/(ASCE)ST.1943-541X.0000178

Chen, S., Fan, C., and Wang, H. (2011). "Experimental study on lateral stiffness of wood shear walls and diaphragms," *Acta Scientiarum Naturalium Universitatis Sunyatseni* 50(4), 42-49. (in Chinese)

Di, J. (2019). *The Lateral Performance of End Panels Strengthed Timber-shear wall under Monotonic Load*, MSc thesis, Northeast Forestry University, Harbin, China. (in Chinese)

Di, J., and Zuo, H. (2021a). "Lateral performance of panel-frame connections in new-type strengthened light wood framed shear walls," *Journal of Northeast Forestry University* 49(4), 81-84. DOI: 10.13759/j.cnki.dlxb.2021.04.015 (in Chinese)

Di, J., and Zuo, H. (2021b). "Experimental and reliability-based investigation on sheathing-to-framing joints under monotonic and cyclic loads," *Forests* 12(8), 995. DOI: 10.3390/f12080995

Di, J., and Zuo, H. (2021c). "Lateral loading performance of end narrow panel reinforced light wood frame shear walls," *International Journal of Structural Integrity* 12(5), 729-742. DOI: 10.1108/IJSI-09-2020-0089

Di, J. (2023). *Lateral Performance of Light Wood Frame Shear Walls Strengthened with Bamboo Scrimber Panels*, Ph.D. Dissertation, Northeast Forestry University, Harbin, China. (in Chinese)

Dong, L., Zheng, W., Zhou, A., Wang, Z., Zhang, L., Ling, Z., and Wang, J. (2023). "Experimental investigation of the lumber-ply bamboo-lumber screwed connections used in midply shear walls," *Construction and Building Materials* 370, article 130656. DOI: 10.1016/j.conbuildmat.2023.130656

Guo, T. (2022). *Lateral Resistance Performance Analysis and Performance Improvement Technology Research of Chuan-Dou Style Wooden Structure*, Ph.D. Dissertation, Beijing Jiaotong University, Beijing, China. (in Chinese)

Guo, T., Yang, N., Zhou, H. and Wang, S. (2022). "Experimental and numerical studies on the traditional penetration mortise–tenon connection reinforced by self-tapping screws," *Forests* 13(4), 513. DOI: 10.3390/f13040513

Li, Z., Xiao, Y., Wang, R., and Shan, B. (2013). "Experimental studies of light-weight woodframe shear walls with ply-bamboo sheathing panels," *Journal of Building Structures* 34(9), 142-149. DOI: 10.14006/j.jzjgxb.2013.09.018 (in Chinese)

Li, H. (2018). *Study on Suitable Strengthening for Ancient Timber Buildings*, Ph.D. Dissertation, Southeast University, Nanjing, China. (in Chinese)

Li, H., Qiu, H., and Wang, W. (2021). "Experimental study on the mechanical performance of mortise-tenon joints reinforced with replaceable flat-steel jackets,"

Journal of Renewable Materials 9(6), 1110-1125. DOI: 10.32604/jrm.2021.014722

Pan, Y., An, R., Wang, X., and Guo, R. (2020). "Study on mechanical model of through-tenon joints in ancient timber structures," *China Civil Engineering Journal* 53(4), 61-70, 82. DOI: 10.15951/j.tmgcxb.2020.04.007 (in Chinese)

Pan, Y., An, R., Chen, J., and Zhang, Q. (2022). "Study on mechanical model of column footing in ancient timber structure based on rocking column," *Journal of Building Structures* 43(6), 196-206. DOI: 10. 14006/ j. jzjgxb. 2020. 0737 (in Chinese)

Pan, Y., An, R., You, W., and Fan, Y. (2023). "A mechanical model used for the multifactor analysis of through-tenon joints in traditional Chinese timber structures," *International Journal of Architectural Heritage* 1-26, DOI: 10.1080/15583058.2023.2173106

Wang, R., Xiao, Y., and Li, Z. (2017). "Lateral loading performance of lightweight glubam shear walls," *Journal of Structural Engineering*, 143(6), article 04017020. DOI: 10.1061/(ASCE)ST.1943-541X.0001751

Wang, R. (2019). *Research on Lightweight Glubam Frame Structures*, Ph.D. Dissertation, Hunan University, Changsha, China. (in Chinese)

Wang, R., Wei, S., Li, Z., and Xiao, Y. (2019). "Performance of connection system used in lightweight glubam shear wall," *Construction and Building Materials* 206, 419-431. DOI: 10.1016/j.conbuildmat.2019.02.081

Xia, T., Zhou, Y., Zheng, W., Dong, L., Wang, Z., and Zhao, T. (2022). "Failure mode and damage assessment of the midply-bamboo shear walls," *Journal of Forestry Engineering* 7(3), 53-59. DOI: 10.13360/j.issn.2096-1359.202109018 (in Chinese)

Xu, Q., Liu, Q., Zhang, F., and Gong, C. (2015). "Experimental research on seismic performance of mortise-tenon joint wood frame with brick masonry infilled wall," *Building Structure* 45(6), 50-53, 49. DOI:10.19701/j.jzjg.2015.06.011 (in Chinese)

Yang, Q., Yu, P., and Law, S. (2020). "Load resisting mechanism of the mortise-tenon connection with gaps under in-plane forces and moments," *Engineering Structures* 219, article 110755. DOI: 10.1016/j.engstruct.2020.110755

Yu, P., Yang, Q., and Law, S. (2021). "Lateral behavior of heritage timber frames with loose nonlinear mortise-tenon connections," *Structures* 33, 581-592. DOI: 10.1016/j.istruc.2021.04.061

Yu, P. (2022). *Lateral Mechanical Performance Analysis of Typical Traditional Wooden Structures*, Ph.D. Dissertation, Chongqing University, Chongqing, China. (in Chinese)

Yu, P., Yang, Q., and Law, S. (2022a). "Lateral performances of traditional wooden frame with loose penetrated mortise-tenon connection and column foot models," *Journal of Building Engineering* 47, article 103793. DOI: 10.1016/j.jobe.2021.103793

Yu, P., Yang, Q., Law, S. and Liu, K. (2022b). "Seismic performances assessment of heritage timber frame based on energy dissipation," *Journal of Building Engineering* 56, article 104762. DOI: 10.1016/j.jobe.2022.104762

Zheng, W., Lu, W., Liu, W., and Liu, X. (2016a). "Lateral force resistance performance of sheathing sandwiched wood shear walls," *Journal of Vibration and Shock* 35(19), 94-100. (in Chinese)

Zheng, W., Lu, W., and Liu, W. (2016b). "Lateral performance and force mechanism of sheathing sandwiched wood shear walls," *of Nanjing Tech University (Natural Science Edition)* 38(5), 13-20 . DOI: 10.3969/j.issn.1671-7627.2016.05.003 (in Chinese)

Zheng, W., Li, Y., Zhou, Y., and Liu, W. (2020). "Experimental investigation on behavior of lumber-ply bamboo-lumber double-shear screwed connections," *Journal of Huazhong University of Science and Technology (Natural Science Edition)* 48(11), 102-108. DOI：10.13245/j.hust.201117 (in Chinese)

Zheng, W., Zhou, Y., and Li, Y. (2021). "Loading behavior and failure mechanism of ply bamboo-sheathed double-shear screwed connections," *Journal of Central South University of Forestry & Technology* 41(7), 156-164. DOI:10.14067/j.cnki.1673-923x.2021.07.019 (in Chinese)

Zheng, W., Zhou, Y., Zhou, A., Dong, L., Lu, W., and Wang, Z. (2023) "Experimental study on lateral performance of the midply-bamboo shear walls," *Journal of Central South University (Science and Technology)* 54(1), 305-313. DOI: 10.11817/j.issn.1672-7207.2023.01.028 (in Chinese)

Zuo, H., and Di, J. (2021). "Experiments and reliability analysis on frame-to-sheathing joints in light wood framed shear walls," *Wood Research* 66(5), 844-858. DOI: 10.37763/wr.1336-4561/66.5.844858

Article submitted: February 16, 2024; Peer review completed: March 16, 2024; Revised version received and accepted: March 17, 2024; Published: March 21, 2024.
DOI: 10.15376/biores.19.2.2916-2934